Flip-Flop-Induced Relaxation of Bending Energy: Implications for Membrane Remodeling

R. J. Bruckner,[†‡‖] S. S. Mansy,[†‡‖] A. Ricardo,[†‡‖] L. Mahadevan,[§¶] and J. W. Szostak[†‡‖*]

[†]Howard Hughes Medical Institute, [‡]Department of Genetics, and [§]Department of Systems Biology, Harvard Medical School, Boston, Massachusetts; [¶]School of Engineering and Applied Sciences, Harvard University, Cambridge, Massachusetts; and [‖]Department of Molecular Biology, Massachusetts General Hospital, Boston, Massachusetts

ABSTRACT Cellular and organellar membranes are dynamic materials that underlie many aspects of cell biology. Biological membranes have long been thought of as elastic materials with respect to bending deformations. A wealth of theory and experimentation on pure phospholipid membranes provides abundant support for this idea. However, biological membranes are not composed solely of phospholipids—they also incorporate a variety of amphiphilic molecules that undergo rapid transbilayer flip-flop. Here we describe several experimental systems that demonstrate deformation-induced molecular flip-flop. First we use a fluorescence assay to track osmotically controlled membrane deformation in single component fatty acid vesicles, and show that the relaxation of the induced bending stress is mediated by fatty acid flip-flop. We then look at two-component phospholipid/cholesterol composite vesicles. We use NMR to show that the steady-state rate of interleaflet diffusion of cholesterol is fast relative to biological membrane remodeling. We then use a Förster resonance energy transfer assay to detect the transbilayer movement of cholesterol upon deformation. We suggest that our results can be interpreted by modifying the area difference elasticity model to account for the time-dependent relaxation of bending energy. Our findings suggest that rapid interleaflet diffusion of cholesterol may play a role in membrane remodeling in vivo. We suggest that the molecular characteristics of sterols make them evolutionarily preferred mediators of stress relaxation, and that the universal presence of sterols in the membranes of eukaryotes, even at low concentrations, reflects the importance of membrane remodeling in eukaryotic cells.

INTRODUCTION

Elastic membrane models have been a central organizing concept in membrane biophysics for more than 35 years. The spontaneous-curvature model first proposed by Canham (1) and Helfrich (2) treats biological membranes as purely elastic with respect to bending. Later experimental observations of vesicle shape transformations led to the development of the area difference elasticity (ADE) model (3):

$$W \equiv \frac{\kappa}{2}\oint dA[C_1 + C_2 - C_0]^2 + \frac{\bar{\kappa}}{2}\frac{\pi}{AD^2}(\Delta A - \Delta A_0)^2.$$

This model's success at predicting membrane behavior is due to its ability to make explicit several individual contributions to the elastic energy of a deformed bilayer. This concept has been substantiated by years of experimentation on pure phospholipid membranes (4). In the ADE model, two factors contribute to the energetics of a curved membrane surface. Taken from the spontaneous-curvature model is the idea that the packing of individual lipid molecules of a given size and shape into two surface layers of opposite curvature necessarily leads to a major percentage of those molecules filling a space for which their inherent geometry is not a perfect match. This contribution is represented by the spontaneous curvature term, C_0, a constant whose value is determined by the identities and quantities of lipids in each monolayer. Second, when a membrane is bent, the negatively curved membrane leaflet is compressed, whereas the positively curved leaflet is expanded. These in-plane area changes give rise to a density disequilibrium across the bilayer, such that the number of molecules in each leaflet does not perfectly correspond to the area of each monolayer. The second term of the ADE model gives the energy contribution due to this effect. Since the energetic barrier for the flipping of phospholipids from one leaflet to another is high, there is no direct mechanism whereby the resulting differential densities of the two deformed leaflets may equilibrate on biological timescales. For biological membranes, the situation is complicated by the presence of a variety of amphiphilic molecules, such as cholesterol, that are known to engage in rapid transbilayer flip-flop (5). This flip-flop provides a time-dependent pathway for the relaxation of differential density-based stress accumulated during membrane bending. We will henceforth refer to this flip-flop-mediated decay of the transbilayer density gradient as ''stress relaxation''. We note that because in vivo membrane remodeling processes, such as endocytosis, are slow relative to cholesterol flip-flop, the transbilayer redistribution of cholesterol is likely to impact the energetics of this biological remodeling process.

Because of the potential relevance of flip-flop to biological processes, we sought to develop methods that would allow the detection of transbilayer movement of diffusible molecules. To that end, we developed three separate model membrane systems. First, we generate fatty acid vesicles

Submitted February 23, 2009, and accepted for publication September 14, 2009.

*Correspondence: szostak@molbio.mgh.harvard.edu

S. S. Mansy's present address is Center for Integrative Biology, University of Trento, Trento, Italy.

Editor: Reinhard Lipowsky.

0006-3495/09/12/3113/10 $2.00

doi: 10.1016/j.bpj.2009.09.025

incorporating the fluorescent dye Laurdan. By reporting the density of lipid packing, Laurdan provides a direct measure of the kinetics of flip-flop-mediated stress relaxation when these vesicles are osmotically deformed in a stopped-flow fluorimeter. Next, we look at the biologically relevant flip-flop of cholesterol in phospholipid vesicles both at equilibrium and in response to deformation. We use an NMR assay to define the rate of cholesterol interleaflet exchange, and a Förster resonance energy transfer (FRET) assay to show that there is indeed a net flux of cholesterol from the compressed leaflet to the expanded leaflet during membrane deformation. We discuss our findings in terms of the current ADE model, along with the potential for future refinements of this model to take into account the time dependence of the membrane energy that results from dynamic processes such as flip-flop. Finally, we consider the implications of our data for the in vivo membrane remodeling activity endocytosis, and discuss the evolutionary significance of the relation between sterols and membrane remodeling in eukaryotic organisms.

MATERIALS AND METHODS

Vesicle preparation

Vesicles were prepared by thin film resuspension or addition of neat oil to buffered solution (5). Vesicles for fluorimetry experiments were made in 0.2 M bicine buffer (Sigma-Aldrich, St. Louis, MO) at pH 8.5 and 50 mM sucrose (Sigma). The cation used was potassium unless specified otherwise. The amphiphile concentrations in stopped-flow experiments were 10 mM for both fatty acid (NuChek, Elysian, MN) and phospholipid (Avanti Polar Lipids, Alabaster, AL), with Laurdan (Fluka, Buchs SG, Switzerland) present at a lipid/dye molar ratio of 400:1. The dyes were initially dissolved in chloroform and mixed with the lipids. The solvent was then evaporated under vacuum, and the lipid resuspended in buffer. Vesicles were then collected and extruded through nucleopore (Whatman, Kent, UK) porous membranes until 100 nm low-dispersity populations were produced as previously described (6). Asymmetric insertion of FRET dyes was achieved by adding dyes as concentrated ethanol stocks to preformed vesicles such that they inserted specifically into the vesicle outer leaflet (7).

Stopped-flow kinetics

Stopped-flow spectrofluorimetry was performed using an Applied Photophysics (Surrey, UK) SX.18MV-R fluorimeter equipped with dual emission detection heads. Vesicles were mixed with buffered solutions of indicated sucrose and cation compositions and excited at 364 nm. Emitted light was detected at 440 nm and 480 nm simultaneously with the appropriate bandpass filters (Omega Optical, Brattleboro, VT). General polarization (GP) was calculated as described previously (8): $GP = (EM_{440} - EM_{480})/(EM_{440} + EM_{480})$, where EM is emission intensity. Experiments were performed at 22°C. Vesicles were deformed by mixing with 300 mM sucrose in 0.2 M bicine at pH 8.5.

Paramagnetic NMR

Spectra were acquired on a Varian 400 MHz spectrometer (^{13}C, 100 MHz; ^{31}P, 80 MHz). Vesicles were made with 20 mM phospholipids with a 1:1 molar ratio of 1-palmitoyl-2-oleoyl-*sn*-glycero-3-phosphocholine (POPC) to 1-palmitoyl-2-oleoyl-*sn*-glycero-3-phosphate (POPA), and 6.5 mM 1-^{13}C-dodecanol (Sigma) or 3-^{13}C-cholesterol (Cambridge Isotopes, Andover, MA). No buffer was used, but the solutions were brought to neutral pH by the addition of NaOH. Preparations were repeatedly sonicated before use to generate uniform ~30 nm vesicles. Experiments were conducted at 37°C, and Mn^{2+} was added to a final concentration of 1 mM.

FRET measurements

Fluorimetry was carried out on a Cary Eclipse (Varian, Mulgrave, Australia). To induce deformation, vesicles were mixed with 0.2 M bicine buffer containing 0.1–1.4 M sucrose. Nitrobenzoxadiazole (NBD) and rhodamine dyes were excited at 430 nm, and emissions were detected at 532 nm (F_{donor}) and 588 nm ($F_{acceptor}$). Dehydroergosterol (DHE) and acylated Cascade Blue (ACB) were excited at 315 nm, and emissions were detected at 376 nm (F_{donor}) and 420 nm ($F_{acceptor}$). Because we were measuring very small changes in the extent of FRET, we did not measure FRET efficiency (the decrease in donor emission in the presence of the acceptor) per se; rather, we measured the change in emission ratio $E = F_{acceptor}/F_{donor}$. This measure is more sensitive than the change in FRET efficiency because it incorporates both the decrease in donor emission and the increase in acceptor emission. More significantly, the change in emission ratio is an internally controlled ratiometric measure that can be followed in a single sample as membrane deformation is increased by the addition of osmolyte. The initial emission ratio E_0 was measured for spherical vesicles ($F_{acceptor}/F_{donor}$ [sphere]), and the final emission ratio E_d ($F_{acceptor}/F_{donor}$ [prolate]) was measured after vesicle deflation by osmolyte addition. The fractional change in emission ratio $\Delta E/E_0$ was defined as $(E_d - E_0)/E_0$. The ACB emission at 420 nm was corrected by subtracting the DHE emission at 420 nm, as determined from parallel samples prepared without ACB. The osmolarity of all buffers was measured on a Wescor (Logan, UT) 5500 vapor pressure osmometer.

Synthesis of ACB

Equimolar amounts of Cascade Blue ethylenediamine (Invitrogen) and palmitic anhydride (Sigma) were mixed in dimethylformamide and heated to 55°C for 15 min. Reaction was quantified by thin-layer chromatography and electrospray ionization mass spectrometry. The solvent was evaporated and the product was used without further purification.

RESULTS

Fatty acid relaxation kinetics

We developed a fluorescence-based kinetic assay to monitor the viscoelastic response of deformed membranes on short timescales. The assay is a classic rheological relaxation experiment in which we induce a constant small-amplitude deformation and then measure the stress relaxation response that follows. Initially, we compared pure phospholipid membranes with membranes composed entirely of fatty acids. Fatty acid membranes mimic many of the properties of biological membranes (6), but differ from phospholipid membranes in their dynamic properties (9). Individual fatty acid monomers continuously enter and exit the otherwise stable membranes and flip from one leaflet to another on a timescale of hundreds of milliseconds (10,11). This distinction renders these membranes ideal for rheological and thus dynamical comparisons. To measure the stress relaxation response, we made use of Laurdan, a lipophilic fluorescent dye that can be incorporated into lipid membranes (8) and used to report the relative penetration of water into the membrane interior. Because water penetration into a

membrane is dependent on interlipid spacing, Laurdan can also be used to measure the density of lipid packing in membranes (12). We prepared 100 nm vesicles that contained Laurdan in their membranes, and then osmotically deflated the vesicles by mixing them with hypertonic sucrose buffer. Deflation requires bending the membrane, as the total membrane curvature changes with the altered surface area/volume ratio. We quantified the Laurdan fluorescence response using the GP parameter (13), which corresponds to the hydrophobicity of the probe microenvironment, with low values denoting a nonpolar state and high values indicating an environment of high chemical polarity.

We implemented the above assay in a stopped-flow fluorimeter to compare the responses of fatty acid and phospholipid membranes to bending. In both cases, we observed an initial rapid increase in GP that corresponded to the bending of the membrane upon osmotic deflation and penetration of water into the expanded outer membrane leaflet. As expected for a purely elastic material, phospholipid membranes sustained the elevated GP value well beyond the experimental timescale of 10 s (Fig. 1, *a* and *c*), indicating that phospholipids store the energy of the deformation in the form of a transmembrane density gradient. In contrast, when fatty acid membranes were examined, GP spiked upward, but rapidly decayed to a lower equilibrium value (Fig. 1, *b* and *c*). This decay results from the flip-flop of fatty acid monomers from the compressed to the expanded leaflet, which expels interposing water molecules as the interleaflet packing density reequilibrates.

We tested three qualitative predictions of the hypothesis that the observed relaxation results from fatty acid flip-flop. The first prediction is that the rate of the decay should depend on fatty acid chain length, which is known to correlate with flip-flop rate (10). We tested fatty acids of varying lengths. Single exponential fits to the stress relaxation curves follow the prediction that shorter chain lengths confer faster kinetics (Fig. 1, *c* and *d*). Second, we observed previously that flip-flop of fatty acid monomers across a membrane is accompanied by their action as ionophores: they act to balance pH and charge on each side of the membrane, and achieve this by carrying protons across in one direction and cations across in the opposite direction (10). The rate of fatty acid redistribution from one leaflet to the other is limited by the rate of flip-flop of the fatty acid-cation salt, which is affected by the identity of the monovalent cation, with $Na^+ > K^+ > Rb^+ > Cs^+$. We therefore prepared vesicles in buffers containing each of these cations, and the measured relative relaxation rates corresponded well with pH gradient relaxation rates measured previously (10), as would be expected if flip-flop is rate-determining in this experiment (Fig. 2 *a*). Finally, the relaxation rate should depend on the concentration, within the membrane, of molecules that flip. To test this, we made vesicles of myristoleic acid (MA), which flips rapidly, and varying amounts of the glycerol monoester of MA, which does not flip on the experimental timescale. We observed a linear dependence of relaxation rate on the concentration of MA in the membranes (Fig. 2 *b*).

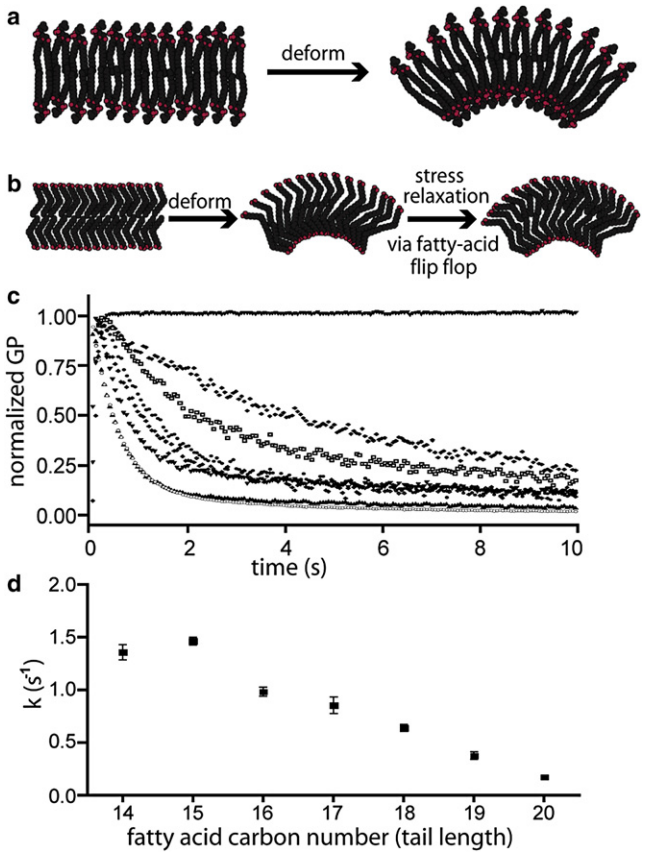

FIGURE 1 Rheological properties of phospholipid and fatty acid membranes. (*a*) Deformation of pure phospholipid membranes results in compression of the inner leaflet and expansion of the outer leaflet. Because phospholipids do not flip-flop on relevant timescales, the energy of the deformation is stored. (*b*) Deformation of fatty acid membranes results in similar compression and expansion of the inner and outer leaflets, but fatty acid monomers rapidly flip from the compressed to the expanded leaflet, resulting in stress relaxation and dissipation of input energy. (*c*) GP determined from Laurdan fluorescence after osmotic stress-induced membrane deformation. POPC membrane GP (*top curve*) increases immediately after membrane deformation and does not decay. Membranes made from seven different monounsaturated fatty acids rapidly relax after deformation, with shorter chain fatty acids showing faster relaxation rates. (◆ C20:1, gondolic acid; □ C19:1, nonadecenoic acid; • C18:1, oleic acid; ◇ C17:1, heptadecenoic acid; ▼ C16:1, palmitoleic acid; ○ C15:1, pentadecenoic acid; ▲ C14:1, MA). (*d*) Relaxation rates determined from the curves shown in panel *c* plotted against the number of carbon atoms in the lipid tail being tested.

Cholesterol interleaflet diffusion

Having demonstrated the flip-flop of fatty acids, we sought to examine membranes more similar to those found in cells. We reasoned that cholesterol is likely to be a key mediator of stress relaxation during membrane remodeling in vivo, because cholesterol is abundant in membranes such as the plasma membrane and synaptic vesicles, which are formed from plasma membrane (mole fraction ~0.4) (14), and because cholesterol was previously shown to flip with

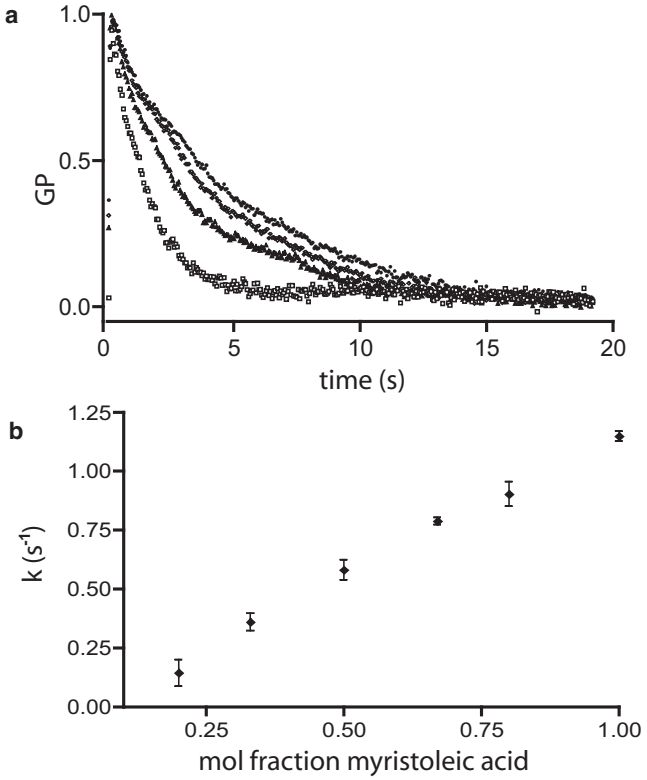

FIGURE 2 Characteristics of fatty acid flip-flop-mediated stress relaxation, showing the correlation between the rate of membrane stress relaxation and the rate of fatty acid interleaflet diffusion (flip-flop). (*a*) Plot of GP versus time after osmotically induced deformation of oleic acid vesicles prepared with different cations. The rate of fatty acid flip-flop is determined by the size of the cation present in the experiment (i.e., smaller cations allow faster flipping). (*Curves*) From bottom to top: Na^+, K^+, Rb^+, and Cs^+. (*b*) Relaxation rate versus mol fraction of fast-flipping MA in mixed MA/glycerol monomyristolein membranes.

a half-time faster than 1 s (5,15), giving ample time for relaxation to occur during the endocytic constriction process. To test the hypothesis that cholesterol may be responsible for membrane stress relaxation, we attempted to observe cholesterol-induced membrane relaxation using the Laurdan stopped-flow assay. However, when we examined cholesterol/phospholipid composite vesicles, we were unable to observe the expected rapid increase and slower decrease in GP. This surprising result led us to hypothesize that stress relaxation had occurred simultaneously with the induced deformation. Since the time constant for vesicle deflation in our assay was ~20 ms, this could only have occurred if cholesterol flip-flop occurs on the millisecond or submillisecond timescale.

To test the hypothesis that rapid cholesterol flip-flop could have prevented the buildup of bending stress in our stopped-flow assay, we developed an NMR-based assay to better define the timescale of cholesterol flip-flop. The assay utilizes paramagnetic NMR to resolve inner- and outer-leaflet contributions to resonance intensity (16). This approach exploits the r^{-6} dependence of dipolar interactions with paramagnetic centers of long electron relaxation times to quench nearby nuclear spins (17). We used Mn^{2+} as the paramagnetic center, which influences the relaxation of nuclei within 25 Å. Since phospholipid membranes are impermeable to Mn^{2+}, and the thickness of the phospholipid bilayer is 30 Å, the addition of Mn^{2+} to the exterior of vesicles rapidly quenches the resonances of lipids that experience the chemical environment of the outer leaflet within the timescale of the experiment. For slowly flipping lipids with half-times of hundreds of milliseconds or longer, this results in the complete quenching of resonances corresponding to outer-leaflet lipids whereas the inner-leaflet resonances are left unaffected. Conversely, for lipids that flip-flop rapidly, every molecule experiences both leaflets within the effective T_2* relaxation time of the nucleus being monitored, and thus complete quenching is observed.

To ensure that this assay reliably gauges lipid flip-flop rates, we measured the effect of Mn^{2+} on the resonances of the slowly flipping phospholipids POPC and POPA, and the rapidly flipping fatty alcohol dodecanol. Under alkaline conditions, the ^{31}P spectrum of POPC/POPA vesicles contains three well-resolved resonances corresponding to POPC (sum of the inner and outer leaflets), inner-leaflet POPA, and outer-leaflet POPA (16). The difference between the more crowded inner-leaflet environment and the less crowded outer-leaflet environment is sufficient to lead to distinct chemical shifts and thus separate, resolvable peaks for inner- and outer-leaflet POPA; however, the phosphorus resonances for inner- and outer-leaflet POPC are not resolved. We reproduced this finding (Fig. 3 *a*) and showed that upon addition of 1 mM Mn^{2+} to the outside of these vesicles, the POPC phosphate peak decreased in intensity by half (as expected from quenching of the outer-leaflet POPC), the outer-leaflet POPA phosphate peak was fully quenched, and the inner-leaflet POPA phosphate peak was unaffected, as expected for molecules that are incapable of flipping on the timescale of the experiment. In contrast, when 1-^{13}C-dodecanol (with a similar T_2*) was incorporated into POPC/POPA vesicles, the observed ^{13}C resonance was fully quenched by the addition of Mn^{2+} (Fig. 3 *b*), consistent with a fast flip-flop rate.

To estimate the flip-flop rate of cholesterol, we prepared POPC vesicles that contained 3-^{13}C-cholesterol, and acquired ^{13}C NMR spectra before and after the addition of Mn^{2+}. Similar to the case of fast-flipping dodecanol, we observed virtually complete quenching of the ^{13}C-cholesterol resonance by 1 mM Mn^{2+} (Fig. 3 *c*). An approximate upper boundary for the timescale of cholesterol flip-flop can be estimated from the linewidths of the ^{13}C-cholesterol spectra in the absence (~1.5 ppm or ~150 Hz) and presence of Mn^{2+} (conservatively 5 ppm or 500 Hz), which correspond to effective T_2* relaxation times of ~2 ms and ~0.6 ms, respectively. As expected, the paramagnetic Mn^{2+} ion leads to faster relaxation, which is evident from the replacement of the initial sharp peak with a much broader low amplitude peak. If cholesterol flips slowly (hundreds of milliseconds), the

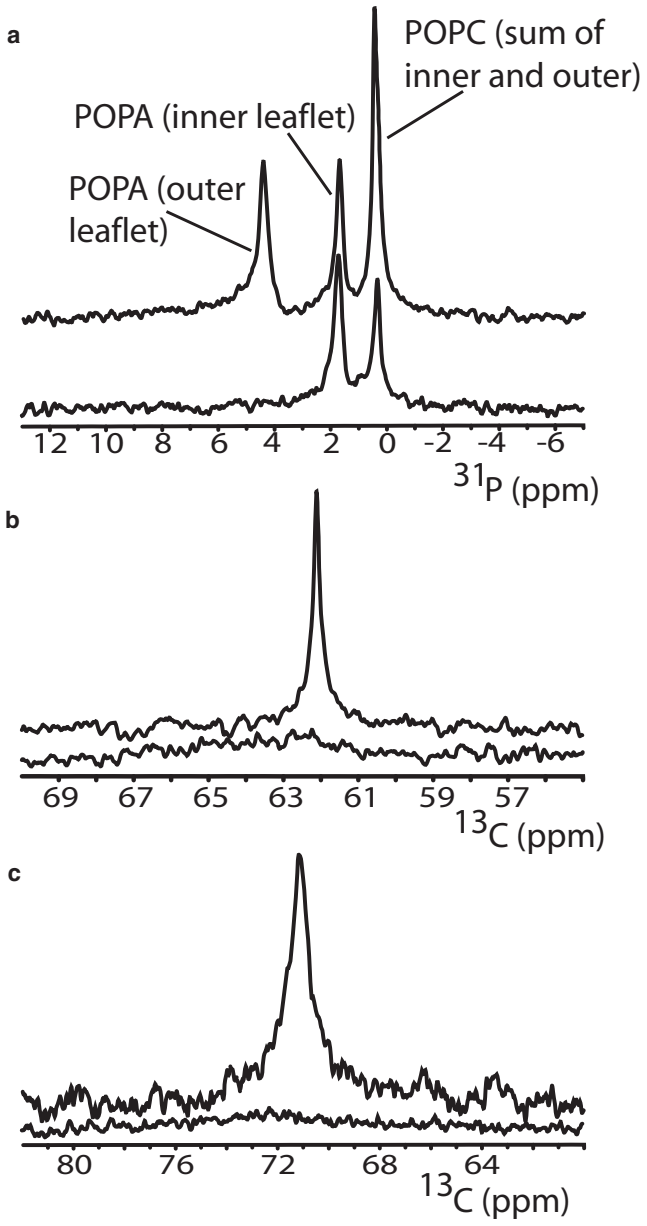

FIGURE 3 Paramagnetic NMR measurement of cholesterol flip-flop. (*a*) ^{31}P NMR of POPC/POPA vesicles demonstrates that addition of Mn^{2+} specifically quenches resonances of outer-leaflet lipids when the lipids flip on a timescale greater than hours. (*b*) ^{13}C NMR of 1-^{13}C-dodecanol reveals that the resonance of both inner- and outer-leaflet dodecanol is quenched due to extremely rapid flip-flop. (*c*) Mn^{2+} addition to POPC vesicles containing 3-^{13}C-cholesterol completely quenches the ^{13}C-cholesterol resonance, showing that all cholesterol in the membrane has experienced the chemical environment of the outer leaflet within the decay time of the NMR signal.

inner-leaflet ^{13}C-cholesterol molecules would not have experienced the Mn^{2+}-containing environment of the outer leaflet within their effective T_2* relaxation time of 2 ms, and would have contributed to a residual sharp peak of linewidth 150 Hz with half the amplitude of the original peak (analogous to the case of POPC above). The simplest interpretation of our observation of a single broadened peak in the presence of Mn^{2+} is that most inner-leaflet cholesterol molecules flip from the inner leaflet to the outer leaflet during the 2 ms window, resulting in faster apparent relaxation and therefore peak broadening. Since the determination of T_2* from linewidth measurements is an approximation, and not all cholesterol molecules flipped within this time period, we suggest that a conservative upper limit on the residence time of cholesterol in a phospholipid membrane leaflet is $\leq$10 ms. Thus, cholesterol interleaflet diffusion is faster than the rate of membrane deformation in our stopped-flow experiments, and explains why we could not measure the rate of relaxation of bending stress using the Laurdan fluorescence assay discussed above. Cholesterol flip-flop is also fast compared to relevant rates of membrane remodeling in cells, and therefore could in principle contribute to stress relaxation in vivo.

Deformation induces cholesterol migration

The above experiments imply that the relaxation of membrane bending energy is mediated at least in part by the redistribution of lipid from the compressed leaflet (whose effective area has decreased) to the tensed leaflet (whose effective area has increased). How much lipid transfer would occur under such a scenario? Two processes may drive transbilayer lipid migration. First, a lipid that can flip-flop should do so to equalize its concentration in the inner and outer leaflets, that is, cholesterol will migrate according to the transbilayer chemical potential. When a membrane is bent, the inner leaflet is compressed and its components are initially at a higher concentration in molecules per unit area; conversely, molecules in the outer expanded leaflet are initially at a lower concentration, and this concentration difference is expected to decay for molecules that can diffuse between leaflets. Beyond this concentration gradient-driven lipid migration, a second effect may drive additional transbilayer movement of molecules that can flip-flop. For a deformed membrane that consists of both flippable and nonflippable lipids, and in which the concentration gradient of the flippable molecule has gone to zero, it is likely that the elastic stress is not yet fully alleviated. In this case, the energetics of molecular packing interactions may favor the loss of additional molecules from the overcrowded inner leaflet, and a corresponding gain of molecules to fill packing voids in the expanded outer leaflet. As an initial step toward determining whether either or both of these mechanisms are involved in lipid redistribution after membrane bending, we sought to experimentally detect the transbilayer redistribution of cholesterol in response to the deformation of phospholipid membranes.

Before attempting to detect cholesterol interleaflet migration, we first sought to measure the relative area change of the outer leaflet of a vesicle after deflation. To do this, we used the distance dependence of FRET between donor and acceptor fluorescent dyes specifically placed in the vesicle outer leaflet. POPC vesicles were formed in the absence of FRET dyes and extruded to 100 nm. To these vesicles

were added the commonly used FRET donor di-oleoyl-phosphatidyl-ethanolamine-NBD (DOPE-NBD) and the acceptor dye DOPE-rhodamine from concentrated ethanol stocks. With this method, externally introduced dyes add only into the outer leaflet of the preformed vesicles because they do not flip across the bilayer (7). These vesicles were then deflated in buffer containing increasing amounts of sucrose. The reduced volume (2) is found by taking the ratio of the osmolality of the surrounding solution to the osmolality of the vesicle interior before sucrose addition (Osm_{out}/Osm_{in}). FRET was measured as the ratio of the acceptor emission ($F_{acceptor}$) to donor emission (F_{donor}) both before and after deflation. A comparison of ''before and after'' FRET values showed that FRET decreased as a function of reduced vesicle volume. This observation is consistent with the predicted increased area of the outer leaflet as a result of deformation: FRET decreases as the increasing outer leaflet area spaces the FRET dyes farther apart.

To relate the observed FRET changes to membrane area changes, we produced a standard curve based on vesicles prepared with differing concentrations of externally added FRET dyes to relate the dye spacing to FRET. To make the standard curve, we prepared unlabeled POPC vesicles and then added FRET dyes to the outer leaflet of these vesicles. After the addition of each aliquot of the dyes, we determined the ratio of acceptor to donor emission intensity. The standard curve (Fig. 4 *a*) shows that as the mol fraction of dye in the membrane increases, FRET increases. The mol fraction of dye in the membrane is equivalent to the intermolecular spacing of the dyes (i.e., as the mol fraction increases, the intermolecular spacing decreases). Because of this relation, the mol fraction is related to the membrane area. Fitting the standard curve with a single exponential, we derived a relationship that allowed us to convert experimentally measured FRET values to the relative membrane area. We used this equation to convert FRET values measured before and after deflation to calculate relative outer leaflet area changes induced by the deflation (Fig. 4 *b*). We then compared the measured area changes with values calculated for an idealized model in which spherical vesicles deflate to adopt a prolate spheroid shape (*line* in Fig. 4 *b*, and supplementary information I text and Fig. S1 in the Supporting Material). Such a shape approximates that observed previously for the deflation of large phospholipid/cholesterol composite vesicles (18). Control experiments in which both FRET dyes were present on both leaflets show no change in FRET after vesicle deflation, consistent with roughly equal and opposite changes in dye spacing in the inner compressed and outer expanded leaflets (Fig. 4 *b*). The correspondence of the experimentally measured area changes with the calculated changes suggests that our model is a reasonable approximation of deflation-induced effects on the vesicle and its membrane at the mesoscopic scale.

Next, we extended the deflation experiment described above to a related scenario in which the FRET donor dye

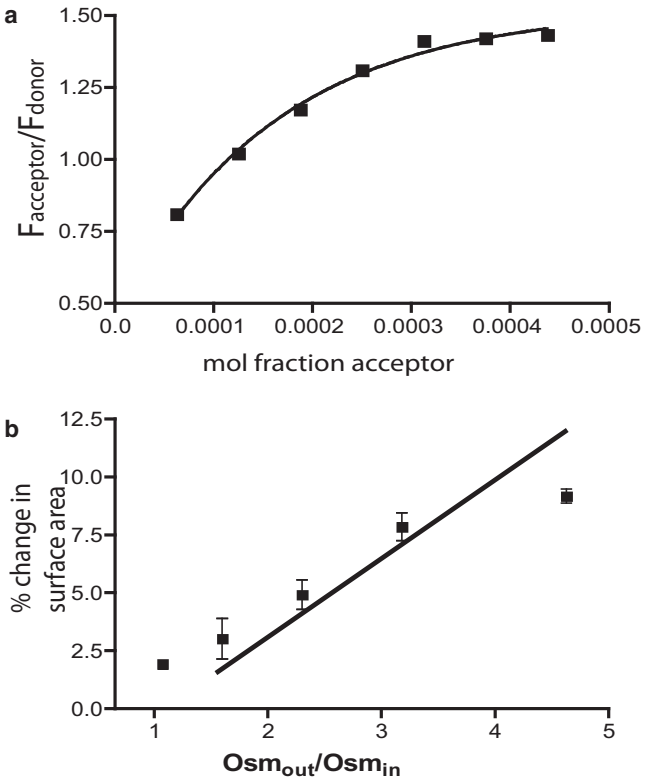

FIGURE 4 Changes in leaflet area after membrane deformation. (*a*) Standard curve relating FRET acceptor emission/donor emission to the mol fraction of acceptor dye added to the vesicle outer leaflet. (*b*) Areal expansion of the outer leaflet of a POPC membrane as a function of osmotic vesicle deflation to the indicated reduced volume fraction. (■) Surface area change as measured by the change in FRET between phospholipid-anchored donor (DOPE-NBD) and acceptor (DOPE-rhodamine) dyes localized to the outer leaflet. (*Solid line*) Change in surface area as calculated for the transition from an initially spherical vesicle to a prolate spheroid after osmotic deflation.

is localized in both leaflets and the FRET acceptor dye is localized specifically in the outer leaflet. This was done to allow us to determine the impact that a nonflipping donor dye localized to the vesicle inner leaflet would have on FRET changes during deflation. These data will be used for comparison with experiments incorporating an inner-leaflet localized flippable FRET donor later on. In this version of the experiment, we formed vesicles in the presence of the FRET donor dye. This gave us vesicles with the FRET donor in both the inner and outer leaflets. To these vesicles we added the FRET acceptor so that it would localize specifically to the outer leaflet. As above, FRET values for these vesicles were measured before and after deflation in sucrose buffers of increasing osmolarity, and, as before, a continuous linear decrease in FRET as a function of increasing outer leaflet area was observed (Fig. 5 *a*). Here, ''before and after'' changes were computed directly from the fractional change in the acceptor/donor emission FRET ratio $\Delta E/E_0$ because it is not possible to generate a standard curve with the asymmetric dye arrangement (see Materials and Methods). Essentially, this experiment tells us that when

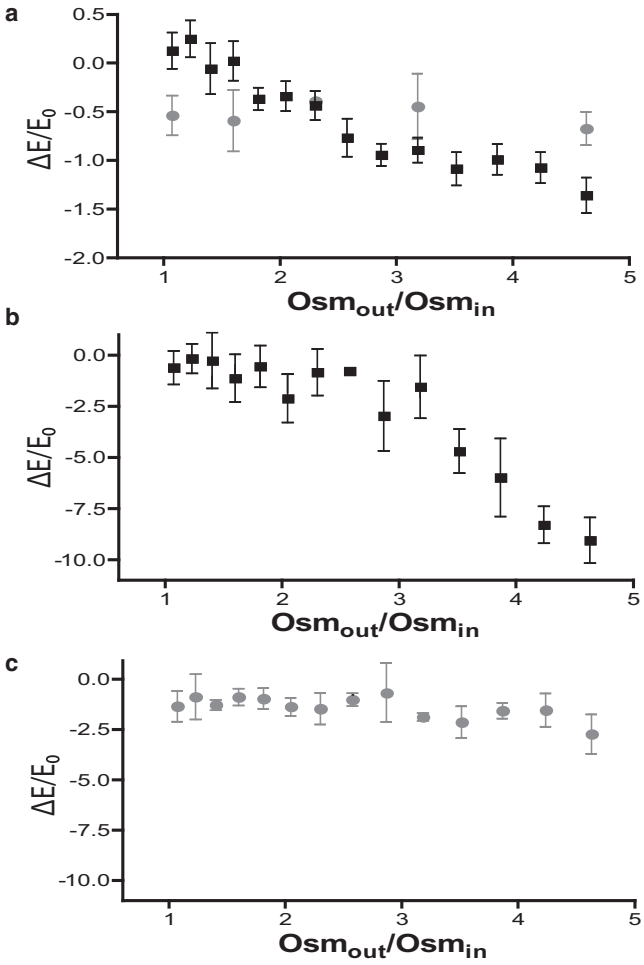

FIGURE 5 Changes in leaflet area after membrane deformation. (*a*) Change in FRET versus deformation when nonflipping phospholipid-labeled FRET dyes are symmetrically or asymmetrically arranged. (■) Donor (DOPE-NBD) present in inner and outer leaflets, acceptor (DOPE-rhodamine) present only in the outer leaflet. With increasing deformation, spacing of outer-leaflet dyes increases and FRET decreases. (*Gray solid circle*) Both dyes present on both leaflets. The FRET decrease due to outer-leaflet expansion balances the FRET increase due to inner-leaflet compression, leading to no net change in the total FRET efficiency. (*b*) Transbilayer redistribution of DHE after vesicle deflation. The FRET donor (DHE) is initially present in both inner and outer leaflets, and can rapidly flip-flop. The FRET acceptor, ACB, is present only in the outer leaflet. For 1% DHE (■), deflation-induced transbilayer redistribution offsets the increased spacing of the outer leaflet dyes until extreme deformations ($Osm_{out}/Osm_{in} > 2.5$, or Δ surface area > 5%), above which the FRET decreases with increasing deformation. (*c*) For vesicles with 1% DHE and 29% cholesterol (*gray solid circle*), flip-flop of cholesterol damps changes in FRET even at extreme deformations.

a nonflipping FRET donor is present in the vesicle inner leaflet, a linear relation can still be observed between the measured FRET change and the outer-leaflet area change.

We then used a similar experimental arrangement to test whether cholesterol migrates across a bilayer after the imposition of membrane-bending stress. First, we generated POPC vesicles that incorporate the fluorescent cholesterol analog DHE. DHE is present during the formation of these vesicles so that it partitions into both inner and outer leaflets. DHE acts as a FRET donor in this system, so this scenario is equivalent to our previous experiment with a FRET donor in both leaflets. We then added a FRET acceptor to the outer leaflet of these vesicles in the same manner as described above. As acceptor, we used a variant of the dye Cascade Blue, which we modified by adding a lipid tail so that it could be localized to the membrane. We call this FRET acceptor ACB. POPC vesicles were made with 1 mol % DHE distributed between the inner and outer leaflets, and ~.25 mol % ACB (~4:1 molar ratio) was then added into the outer leaflet. FRET was measured for these vesicles in the same way as described above, i.e., FRET was measured before and after deflation, and the values were compared to generate data in the form of the fractional change, $\Delta E/E_0$. (Fig. 5 *a*). The resulting profile for $\Delta E/E_0$ versus deflation differs markedly from the control experiment using the nonflipping phospholipid-linked FRET dyes above (compare Fig. 5, *a* and *b*). Instead of a linear response, the DHE/ACB system shows no change in FRET until a reduced volume of ~0.4 is reached, corresponding to a 5% increase in outer-leaflet area (Fig. 5 *b*). Beyond this point, $\Delta E/E_0$ decreases sharply.

Why is there no change in the degree of FRET for the DHE/ACB dyes until an outer-leaflet area change of >5% occurs? This observation is in clear contrast to the continuous decrease in FRET with vesicle deflation that was observed using two nonflipping phospholipid-conjugated dyes. The simplest interpretation of this effect is that it is a consequence of the transfer of DHE from the inner to the outer leaflet as DHE equilibrates in response to the imposed chemical potential by flowing from the compressed inner leaflet to the expanded outer leaflet. This redistribution of DHE would maintain a constant FRET donor concentration in the outer leaflet, and thus a constant efficiency of FRET to the outer-leaflet localized ACB acceptor dye. Recent work from two groups (19,20) provides perhaps the best indication of the extent of cholesterol redistribution that occurs in response to small-scale deformation. In experiments aimed at evaluating the extent to which lipids will laterally sort on the basis of curvature, these groups found that lipids will concentrate only in the event that bulk phase separation takes place. Without this condition, entropy-driven mixing dominates over the energetic benefit of arranging molecules within the bilayer to match curvature with molecular geometry. In our experiments, vesicles are composed of just two lipid types and are perfectly mixed. Therefore, we expect that cholesterol concentration across the bilayer will equilibrate. Flip-flop of cholesterol past this concentration equilibrium is unlikely.

At greater deformations, corresponding to outer-leaflet area changes >5%, $\Delta E/E_0$ does decrease (Fig. 5 *b*). This decline may be due to the fact that by ~5% area expansion, all of the DHE has already flipped to the outer leaflet, so that further expansion of the outer leaflet must lead to increased distance between the dye molecules and a pronounced drop in $\Delta E/E_0$. In this case, the extreme area imbalance appears to

have created an elastic situation of sufficiently high energy to dominate the entropic tendency of DHE to equilibrate its concentration across and within leaflets. To test this hypothesis, we produced vesicles containing the same arrangement of DHE and ACB, and, in addition, 29 mol % cholesterol in both leaflets. The incorporation of 29% cholesterol into the 1% DHE vesicles does not affect the region of constant FRET (for a <5% area change), but it does largely damp the observed FRET changes for larger deformations ($Osm_{out}/Osm_{in} > 3.5$; Fig. 5*c*). Since DHE and cholesterol can both flip, for small deformations they will both do so until the inner- and outer-leaflet areal concentrations have become equalized and therefore no change is seen in FRET. However, at large membrane deformations (for a >5% area change), their combined transbilayer redistribution relaxes the stored elastic energy that drives the excess migration of DHE seen in the absence of cholesterol. Our results suggest that the transbilayer redistribution of sterols, including cholesterol, leads to the relaxation of some membrane-bending stress, but the extent of relaxation may be limited to the decay of the sterol concentration gradient. A more detailed discussion of the theoretical considerations implied in this analysis, as well as those raised by others in the past, is presented in supplementary information II in the Supporting Material.

DISCUSSION

The elastic membrane theory is ubiquitous in theoretical and molecular modeling of biomembrane behaviors ranging from membrane fusion and fission activities (21,22) to protein aggregation (23) and the regulation of certain protein enzymatic activities (24). The issue of flip-flop is often raised in discussions of these biological processes, and yet little has been done to quantitatively assimilate flip-flop into the membrane model. In addition to the work presented here, a number of membrane deformation experiments on reconstituted lipid vesicles have substantiated the idea that the presence of flip-flop alters the standard elastic membrane. Yanagisawa et al. (25) prepared 40 μm unilamellar vesicles composed of a ternary mixture of unsaturated phospholipids, saturated phospholipids, and cholesterol. These membranes exhibit phase separation, with the saturated lipids and cholesterol forming liquid-ordered (l_o) membrane subdomains that segregate from liquid-disordered (l_d) domains composed of the unsaturated phospholids. Each subdomain is specifically fluorescently labeled, and the vesicles are then deflated and viewed with fluorescence and confocal microscopy. The images produced reveal that it is the cholesterol-rich domains that deform in response to the induced deflation, whereas the pure phospholipid domains remain largely unchanged. In contrast, studies in which the bending rigidities of pure phospholipid membranes and phospholipid/cholesterol membranes were measured indicate that it is the addition of cholesterol that increases membrane stiffness (26,27). The preferential deformation of the l_o domain observed by Yanagisawa et al. (25) is therefore puzzling. Because its elastic component is stiffer, we might predict that it would resist deformation whereas the cholesterol-free l_d domain would be deformed. In fact, this illustrates that elasticity is not the sole material property at play in the deformation of a complex membrane—transbilayer flip-flop introduces a viscous property. Thus, the observed preferential deformation of the l_o domains in complex lipid mixtures is likely due to the flip-flop of cholesterol in these domains, which specifically relaxes tension in these regions despite their greater stiffness. In related studies, Bacia et al. (28) observed this same tendency; they commented on the unexpected nature of the finding and reached the same conclusion we have presented here.

In another study, Döbereiner et al. (18) observed budding from sphingolipid and phospholipid vesicles as a result of temperature-induced deformation. Because the lipid bilayers expand more than the water in response to the increased temperature, an area imbalance is generated between the two leaflets that gives rise to an elastic stress. Time-lapse images reveal that this stress is relaxed by the budding of daughter vesicles from the parent membrane. However, when phospholipid/cholesterol composite membranes were tested, budding was not observed. We suggest that this is due to cholesterol flip-flop allowing relaxation of the imposed stress, such that insufficient tension remains to drive budding.

When used to model the fission activity of endocytosis, this model predicts a required energy input of ~500 k_BT to generate the highly curved vesicle neck before vesicle release. The high energies predicted for neck formation and excision have long been considered problematic (29). We suggest that the elastic energy that is built up during endocytosis may be alleviated in part by cholesterol transbilayer redistribution. This notion is consistent with electron microscopy studies of cholesterol-depleted cells that show specific defects in endocytosis in vivo. Rodal et al. (30) and Subtil et al. (31) have each shown that de novo vesicle formation by endocytosis is arrested at preliminary stages of membrane budding upon depletion of cholesterol. In this case, it appears that membrane remodeling associated with the formation of the clathrin-coated pit cannot occur without a cholesterol-mediated stress relaxation mechanism.

The disruption of endocytic vesicle recycling at the synapse is a related case. Synaptic vesicle recycling is distinct from other forms of endocytosis in that the budded state is generally maintained through the fusion and subsequent fission steps (32,33). High-energy membrane bending is therefore localized at the neck region, and we would predict this to be the point of arrest in cholesterol-depleted neurons. The kinetics of endocytosis are likely on the order of ~10–20 s as determined by the rate of action of the protein dynamin (34,35), which is responsible for inducing the excision of the neck of a budding vesicle. Dynamin ablation

results in synaptic vesicles that are increased in size and reduced in number (36), and endocytic events that arrest before excision, accumulate, and give rise to deeply invaginated compartments that fail to mature into vesicles. Recent electron microscopy images (37) of hippocampal neurons depleted of cholesterol reveal a similar phenotype: synaptic vesicles are decreased in number and appear significantly larger, whereas synaptic terminals are lined with arrested endocytic compartments. A compelling explanation is that the transbilayer cholesterol diffusion observed in our experiments applies directly to membrane remodeling in vivo. Taken together, these results suggest that the relaxation of membrane-bending stress is a previously unrecognized feature that accompanies cellular membrane remodeling activities provided that the membranes contain a sterol and that the timescale of remodeling is $>\sim$10 ms.

It is striking that although sterols are major components of the membranes of all eukaryotes, they occur only sporadically among the eubacteria and archaea. We suggest that this reflects the characteristic elaboration of membrane remodeling processes among eukaryotic organisms, combined with the biophysically relevant properties of the sterols. Sterols optimize the packing of lipids above their T_m, thereby stiffening such membranes and at the same time enabling their deformation at a lower energetic cost. They make membranes less permeable to water and ions, and thus more effectively seal off a cell from its outside environment while at the same time they facilitate endocytosis and thereby enable ligand-specific cellular uptake. Few biological membrane constituents possess this combination of diverse traits. We have shown that fatty acids can mediate stress relaxation of deformed membranes, but that in vivo fatty acids would erode the essential ion and proton gradients that exist across cytoplasmic membranes and synaptic vesicles (8). Fatty alcohols may also mediate stress relaxation, and as uncharged species they would not act as ionophores; however, as single chain amphiphiles, they would not be firmly anchored in the membrane and could not be appropriately localized. Sterols such as cholesterol have a hydrophobic surface area closer to that of phospholipids and are thus firmly anchored in the membrane, and at the same time their small polar headgroup (a single hydroxyl at the 3 position) allows for rapid interleaflet flip-flop. The physical properties of sterols are thus ideal for their role as biological mediators of membrane stress relaxation.

SUPPORTING MATERIAL

Supplementary information I and II, a figure, and references are available at http://www.biophysj.org/biophysj/supplemental/S0006-3495(09)01506-9.

We thank Dan Bruckner, Michael Heymann, Itay Budin, Irene Chen, Na Zhang, and Josh Kaplan for helpful discussions.

This work was supported in part by NASA-Exobiology grant NNX07AJ09G. R.J.B. was supported by a fellowship from the Harvard Origins of Life Initiative. J.W. S. is an investigator at the Howard Hughes Medical Institute.

REFERENCES

1. Canham, P. B. 1970. The minimum energy of bending as a possible explanation of the biconcave shape of the human red blood cell. *J. Theor. Biol.* 26:61–81.
2. Helfrich, W. 1973. Elastic properties of lipid bilayers—theory and possible experiments. *Z. Naturforsch. [C].* 28:693–703.
3. Miao, L., U. Seifert, M. Wortis, and H.-G. Döbereiner. 1994. Budding transitions of fluid bilayer vesicles: the effect of area-difference elasticity. *Phys. Rev. E.* 49:5389–5407.
4. Döbereiner, H.-G., E. Evans, M. Kraus, U. Seifert, and M. Wortis. 1997. Mapping vesicle shapes into the phase diagram: a comparison of experiment and theory. *Phys. Rev. E.* 55:4458–4474.
5. Hamilton, J. A. 2003. Fast flip-flop of cholesterol and fatty acids in lipid membranes: implication for membrane transport proteins. *Curr. Opin. Lipidol.* 14:263–271.
6. Hanczyc, M. M., S. M. Fujikawa, and J. W. Szostak. 2003. Experimental models of primitive cellular compartments: encapsulation, growth and division. *Science.* 302:618–622.
7. Matsuzaki, K., O. Murase, N. Fujii, and K. Miyajima. 1996. An antimicrobial peptide, magainin 2, induced rapid flip-flop of phospholipids coupled with pore formation and peptide translocation. *Biochemistry.* 35:11361–11368.
8. Parasassi, T., G. De Stasio, A. d'Ubaldo, and E. Gratton. 1990. Phase fluctuation in phospholipid membranes revealed by Laurdan fluorescence. *Biophys. J.* 57:1179–1186.
9. Chen, I., R. W. Roberts, and J. W. Szostak. 2004. The emergence of competition between model protocells. *Science.* 305:1474–1476.
10. Chen, I., and J. W. Szostak. 2004. Membrane growth can generate a transmembrane pH gradient in fatty acid vesicles. *Proc. Natl. Acad. Sci. USA.* 101:7965–7970.
11. Kamp, F., D. Dakim, N. Noy, and J. A. Hamilton. 1995. Fatty acid flip-flop in phospholipid vesicles is extremely fast. *Biochemistry.* 34:11928–11957.
12. Söderlund, T., J.-M. Alakoskela, A. L. Pakkanen, and P. K. Kinnunen. 2003. Comparison of the effects of surface tension and osmotic pressure on the interfacial hydration of a fluid phospholipid bilayer. *Biophys. J.* 85:2333–2341.
13. Parasassi, T., G. De Stasio, G. Ravagnan, R. M. Rusch, and E. Gratton. 1991. Quantitation of lipid phases in phospholipid vesicles by the generalized polarization of laurdan fluorescence. *Biophys. J.* 60:179–189.
14. Takamori, S., M. Holt, K. Stenius, E. A. Lemke, M. Grønborg, et al. 2006. Molecular anatomy of a trafficking organelle. *Cell.* 127:831–846.
15. Steck, T. L., J. Ye, and Y. Lange. 2002. Probing red cell membrane cholesterol movement with cyclodextrin. *Biophys. J.* 83:2118–2125.
16. Swairjo, M. A., B. A. Seaton, and M. F. Roberts. 1994. Effect of vesicle composition and curvature on the dissociation of phosphatidic acid in small unilamellar vesicles—a ^{31}P-NMR study. *Biochim. Biophys. Acta.* 1191:354–361.
17. Bertini, I., C. Luchinat, G. Parigi, and R. Pierattelli. 2005. NMR spectroscopy of paramagnetic metalloproteins. *ChemBioChem.* 6:1536–1549.
18. Döbereiner, H.-G., J. Kas, D. Noppl, I. Sprenger, and E. Sackmann. 1993. Budding and fission of vesicles. *Biophys. J.* 65:1396–1403.
19. Sorre, B., A. Callan-Jones, J. B. Manneville, P. Nassoy, J. F. Joanny, et al. 2009. Curvature-driven lipid sorting needs proximity to a demixing point and is aided by proteins. *Proc. Natl. Acad. Sci. USA.* 106:5622–5626.
20. Tian, A., and T. Baumgart. 2009. Sorting of lipids and proteins in membrane curvature gradients. *Biophys. J.* 96:2676–2688.
21. Markin, V. S., and J. P. Albanesi. 2002. Membrane fusion: stalk model revisited. *Biophys. J.* 82:693–712.
22. Kozlovsky, Y., and M. M. Kozlov. 2003. Membrane fission: model for intermediate structures. *Biophys. J.* 85:85–96.
23. Reynwar, B. J., G. Illya, V. A. Harmandaris, M. M. Muller, K. Kremer, et al. 2007. Aggregation and vesiculation of membrane proteins by curvature-mediated interactions. *Nature.* 447:461–464.

24. Davies, S. M., R. M. Epand, R. Kraayenhof, and R. B. Cornell. 2001. Regulation of CTP: phosphocholine cytidylyltransferase activity by the physical properties of lipid membranes: an important role for stored curvature strain energy. *Biochemistry*. 40:10522–10531.

25. Yanagisawa, M., M. Imai, and T. Taniguchi. 2008. Shape deformation of ternary vesicles coupled with phase separation. *Phys. Rev. Lett.* 100:148102.

26. Meleard, P., C. Gerbeaud, T. Pott, L. Fernandez-Puente, I. Bivas, et al. 1997. Bending elasticities of model membranes: influence of temperature and sterol content. *Biophys. J.* 72:2616–2629.

27. Henriksen, J., A. C. Rowat, Y. W. Hsueh, J. L. Thewalt, M. J. Zuckermann, et al. 2006. Universal behavior of membranes with sterols. *Biophys. J.* 90:1639–1649.

28. Bacia, K., P. Schwille, and T. Kurzchalia. 2005. Sterol structure determines the separation of phases and the curvature of the liquid-ordered phase in model membranes. *Proc. Natl. Acad. Sci. USA*. 102:3272–3277.

29. Lentz, B. R., D. P. Siegel, and V. Malinin. 2002. Filling potholes on the path to fusion pores. *Biophys. J.* 82:555–557.

30. Rodal, S. K., G. Skretting, O. Garred, F. Vilhardt, B. van Deurs, et al. 1999. Extraction of cholesterol with methyl-β-cyclodextrin perturbs formation of clathrin-coated endocytic vesicles. *Mol. Biol. Cell*. 10:961–974.

31. Subtil, A., I. Gaidarov, K. Kobylarz, M. A. Lampson, J. H. Keen, et al. 1999. Acute cholesterol depletion inhibits clathrin-coated pit budding. *Proc. Natl. Acad. Sci. USA*. 96:6775–6780.

32. Aravanis, A., J. Pyle, and R. W. Tsien. 2003. Single synaptic vesicles fusing transiently and successively without loss of identity. *Nature*. 423:643–647.

33. Willig, K., S. Rizzoli, V. Westphal, R. Jahn, and S. Hell. 2006. A membrane marker leaves synaptic vesicles in milliseconds after exocytosis in retinal bipolar cells. *Nature*. 440:935–939.

34. Sever, S., H. Damke, and S. L. Schmid. 2000. Dynamin:GTP controls the formation of constricted coated pits, the rate limiting step in clathrin-mediated endocytosis. *J. Cell Biol*. 150:1137–1147.

35. Roux, A., K. Uyhazi, A. Frost, and P. De Camilli. 2006. GTP-dependant twisting of dynamin implicates constriction and tension in membrane fission. *Nature*. 441:528–531.

36. Ferguson, S. M., G. Brasnjo, M. Hayashi, M. Wölfel, C. Collesi, et al. 2007. A selective activity-dependent requirement for dynamin 1 in synaptic vesicle endocytosis. *Science*. 316:570–574.

37. Wasser, C. R., M. Ertunc, L. Xinran, and E. T. Kavalali. 2007. Cholesterol-dependent balance between evoked and spontaneous synaptic vesicle recycling. *J. Physiol*. 579:413–429.